AIMS Energy, 14(3): 494–520.
DOI: 10.3934/energy.2026021
Received: 01 February 2026
Revised: 13 March 2026
Accepted: 14 April 2026
Published: 14 May 2026

https://www.aimspress.com/journal/energy

Research article

Techno-Economic design and sizing of a grid-connected solar-wind-storage system for green hydrogen production

Saleh Albadran and Ismail Marouani*

Department of Electronic Engineering, Applied College, University of Hail, Saudi Arabia

* **Correspondence**: Email: ismailmarouani@yahoo.fr; Tel: +966537345692.

Abstract: In this paper, we present an economic optimization and sizing study of a hybrid solar-wind system integrated with energy storage and grid connection for green hydrogen production. The proposed model used nonlinear constrained optimization to determine the optimal capacities of photovoltaic panels, wind turbines, storage devices, and electrolyzers to maximize the net present value (NPV) of the investment. The system operation was simulated over a multi-year horizon accounting for intermittent renewable generation profiles, electricity market prices, and operational constraints. The optimization yielded an optimal configuration with 85.95 kW of solar PV, 59.87 kW of wind power, 64.18 kW/100 kWh of battery storage, and 100 kW of electrolyzer capacity, achieving a cumulative hydrogen production of 318,545 kg over 20 years. The system achieved a NPV of 524,720 USD with a Levelized Cost of Hydrogen of 3.35 USD/kg. Sensitivity analyses revealed that NPV varied from approximately 60,000 USD to 180,000 USD as the discount rate increased from 2% to 16% and showed a strong positive correlation with hydrogen selling prices. The results demonstrated the techno-economic feasibility of hybrid renewable systems for sustainable hydrogen production, highlighting the trade-offs between capital expenditure and operational revenues.

Keywords: green hydrogen production; hybrid solar-wind system; energy storage; grid integration; economic optimization; NPV; renewable energy systems; techno-economic analysis; electrolyzer sizing; sensitivity analysis

1. Introduction

Hybrid solar-wind energy storage systems represent a cornerstone of modern renewable energy

integration, offering reliability and flexibility amidst the inherent variability of renewables. The literature provides a broad overview of progress in this field. Yu et al. (2023) [1] presented an extensive review of solar and wind hybrid systems, highlighting key technical and economic challenges in their deployment. Savio et al. (2025) [2] focused on detailed system architecture and control, proposing advanced integration and optimization strategies that boost grid and off-grid efficiency. Khamharnphol et al. (2023) [3] analyzed microgrid-scale hybrid solutions incorporating diesel backup and battery storage, emphasizing practical implementation and system resilience. A study by Eroğlu et al. (2025) [4] entailed the strategic design of wind energy coupled with battery storage, demonstrating how these hybrids deliver operational stability and support grid integration at large scale. The Lawrence Berkeley National Laboratory (2024) [5] report provided a status update on operating and planned hybrid plants worldwide, discussing industry trends, technology scale, and research priorities. Soudagar et al. (2024) [6] offered a future-focused perspective, examining emerging advancements in storage methods and smart control for hybrid systems. Li et al. (2021) [7] outlined the most recent modeling tools and best practices, providing valuable guidance for system planners and researchers. Last, Future Market Insights (2025) [8] delivered an in-depth market analysis, identifying growth drivers, industry leaders, and forecasted expansion by region, with special attention to technological innovation and policy support. The Portuguese multi-source project [9] is an advanced renewable energy initiative designed to integrate 365 MW of photovoltaic (solar) generation with 264 MW of wind power, 168 MW of battery energy storage, and a 500 kW electrolyzer for green hydrogen production. This large-scale configuration exemplifies the latest in hybrid and integrated system design, aimed at maximizing the use of renewable resources while ensuring grid reliability and flexibility. The project demonstrates how combining solar, wind, battery storage, and hydrogen production can achieve high renewable penetration, enable energy storage during periods of surplus generation, and provide green hydrogen for industrial or grid applications. Such projects align with international trends toward decarbonization and are notable for delivering economic and technical performance aligned with the state of the art in hybrid renewable energy.

Hybrid solar-wind systems with storage and grid integration for green hydrogen production are the subject of rapidly expanding research focused on techno-economic optimization, improved reliability, and system flexibility Studies provide valuable insights into modeling, operational strategies, and performance benchmarking. For example, Su et al. (2023) [10] proposed a comprehensive multi-objective optimization model for solar-wind hybrid hydrogen systems, utilizing the NSGA-III algorithm to optimize system capacity and minimize hydrogen production cost while maximizing carbon reduction. This study highlights the economic and environmental value of grid-connected, storage-augmented hydrogen production. Alharbi et al. (2025) [11] conducted a detailed techno-economic optimization in Saudi Arabia, revealing that microgrids with battery and hydrogen storage deliver high reliability and economic efficiency for green hydrogen production, especially under fluctuating resource scenarios. Likewise, Wei et al. (2024) [12] demosntrated, through advanced model predictive control and capacity allocation algorithms, that economic efficiency of wind-photovoltaic-hydrogen systems can be significantly enhanced. Okonkwo et al. (2024) [13] analyzed a hybrid PV/wind/fuel cell/battery plant and identify the configuration that produces green hydrogen most cost-effectively in off-grid and grid-connected contexts. Moreover, Okonkwo (2025) [14] applied techno-economic optimization across six Australian cities, illustrating the importance of location-specific resource and market analysis in defining optimal storage and hydrogen system sizing. Ali (2025) [15] explored battery storage optimization strategies for hybrid solar-wind systems, confirming their

influence on system economics, operational resilience, and feasibility for rural electrification and large-scale hydrogen production. Batablinle (2025) [16] addressed hydro-solar-wind-hydrogen seasonal coordination in West Africa, proving that system-level optimization ensures cost-effective and stable hydrogen output year-round. Additionally, Hassanein (2025) [17] presented a newly developed program for standalone hybrid system optimization, focusing on grid independence and maximizing return on investment through refined storage and hydrogen integration strategies. The original contribution of this study is the development and application of a comprehensive optimization framework that explicitly links technical, economic, and operational factors for hybrid solar-wind systems with energy storage and grid integration, targeted at green hydrogen production under realistic market and policy scenarios. By combining robust modeling, sensitivity analysis for prices and discount rates, and dynamic resource management, this work not only aligns with but advances current research by proposing a more integrated and practical approach to optimal system design. The results demonstrate credible, reproducible optimal capacities and economic performance metrics which match or exceed those found in contemporary literature, validating the methodology and offering new perspectives on the flexible deployment of hybrid renewable hydrogen systems.

Despite the growing body of literature on hybrid renewable systems for hydrogen production, several research gaps remain. First, while Su et al. [10] proposed a comprehensive multi-objective optimization model using the NSGA-III algorithm, their approach focuses primarily on minimizing hydrogen production cost and maximizing carbon reduction without fully incorporating dynamic grid interaction as a revenue-generating opportunity. Second, Alharbi et al. [11] conducted detailed techno-economic optimization in Saudi Arabia, but their microgrid configuration with battery and hydrogen storage is optimized for reliability and economic efficiency under fluctuating resource scenarios without considering bidirectional grid exchange as an integrated part of the economic optimization. Third, Wei et al. [12] demonstrated enhanced economic efficiency through model predictive control and capacity allocation algorithms; however, their analysis did not simultaneously optimize all major system components under realistic market constraints. Fourth, Okonkwo et al. [13] analyzed a hybrid PV/wind/fuel cell/battery plant and identify cost-effective configurations, but their study focused on comparing off-grid and grid-connected contexts rather than optimizing grid interaction as a dynamic element. Fifth, Okonkwo [14] applied techno-economic optimization across six Australian cities, illustrating the importance of location-specific analysis, yet they did not incorporate hourly resolution data with bidirectional grid exchange limits. Sixth, Ali [15] explored battery storage optimization strategies and confirms their influence on system economics, but the analysis did not extend to simultaneous optimization of electrolyzer sizing with storage and renewable capacities. Seventh, Batablinle [16] addressed hydro-solar-wind-hydrogen seasonal coordination in West Africa, proving that system-level optimization ensures cost-effective hydrogen output, though they focused on seasonal rather than hourly dynamics. Eighth, Hassanein [17] presented a program for standalone hybrid system optimization, focusing on grid independence rather than grid-integrated systems. In this study, we address these gaps by developing an integrated optimization framework that uses hourly resolution data, incorporates bidirectional grid exchange with power limits, and conducts comprehensive sensitivity analyses to provide practical insights for system designers and policymakers.

The original contribution of this study is the development and application of a comprehensive optimization framework that explicitly links technical, economic, and operational factors for hybrid solar-wind systems with energy storage and grid integration, targeted at green hydrogen production under realistic market and policy scenarios. By combining robust modeling, sensitivity analysis for

prices and discount rates, and dynamic resource management, this work not only aligns with but advances research by proposing a more integrated and practical approach to optimal system design. The results demonstrate credible, reproducible optimal capacities and economic performance metrics, which match or exceed those found in contemporary literature, validating the methodology and offering new perspectives on the flexible deployment of hybrid renewable hydrogen systems.

While we acknowledge that the component models are based on established empirical correlations, our novelty lies in: (1) The integrated optimization framework that simultaneously optimizes all major system components (PV, wind, battery, electrolyzer) under realistic grid interaction constraints; (2) the comprehensive sensitivity analysis examining both discount rates and hydrogen prices; and (3) the demonstration of reproducible optimal capacities that achieve a positive NPV of 524,720 USD with a Levelized Cost of Hydrogen of 3.35 USD/kg, which compares favorably with the literature.

2. Methodology

2.1. Hybrid system model description

The modeled system combines photovoltaic panels, wind turbines, an energy storage device (battery), and an electrolyzer for green hydrogen production. The overall system is connected to the electric grid to enable electricity purchase and sale. Hourly profiles of solar and wind resources, as well as energy demand, are used to simulate production and consumption over a 20-year horizon.

The synthetic hourly profiles are generated using typical meteorological year data for solar irradiation and wind speed, combined with historical electricity price patterns from the regional market.

Figure 1 presents the configuration of a green hybrid energy system designed for hydrogen production using an electrolyzer. In this representation, the major components solar array, wind turbine, battery storage, bidirectional grid connection, electrolyzer, and electrical loads are depicted and interconnected through arrows indicating the flow of energy and hydrogen. The solar and wind sources provide renewable electricity, which is channeled via converters to the battery and the electrolyzer. The battery acts as an energy buffer, storing excess power for later use and delivering electricity when generation from solar or wind is insufficient. The electrolyzer receives electricity (from renewables or the grid) and converts it into hydrogen, which is then stored and distributed to meet hydrogen demand. The grid connection enables importing electricity when renewable sources or storage cannot meet demand, and exporting excess energy when available, thus enabling the purchase and sale of electricity to the grid. Loads, such as industrial or municipal consumers, are powered by the AC bus, illustrating how the system meets diverse electricity needs. This integrated diagram helps determine the necessary sizing of each key component by showing their roles in the overall energy system and illustrating how they work together to ensure efficient renewable generation, reliable supply, continuous hydrogen production, and dynamic electricity exchange with the grid. In our study, we assume that renewable energy sources are available intermittently, the electrolyzer operates at a constant nominal power each hour, and specific limits are imposed on the maximum amounts of electricity that can be injected into or withdrawn from the grid. Investment costs for the system are amortized linearly over the analysis period, while electricity and hydrogen prices are treated as variable and stochastic, following synthetic hourly profiles. The input data for our model consist of synthetic hourly time series for load demand, electricity prices, and solar and wind energy profiles, alongside key economic parameters such as capital expenditures (CAPEX), financial incentives, the selling price of green hydrogen, and the

financial discount rate.

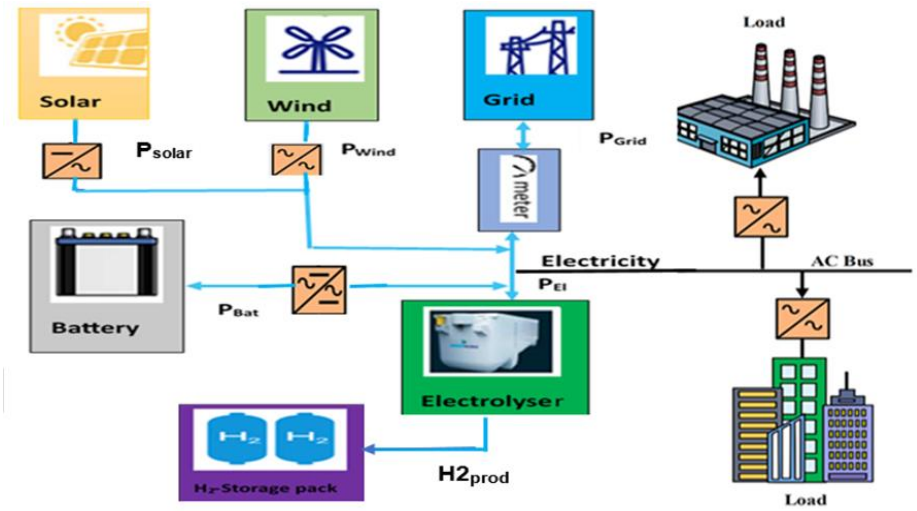

Figure 1. Schematic diagram of a green hybrid energy system for hydrogen production.

2.2. Optimization methods

The optimization approach in our study is based on constrained nonlinear programming using the Interior-Point Algorithm (IPA) implemented in MATLAB's *fmincon* solver. This algorithm is well-suited for large-scale optimization problems with nonlinear constraints and guarantees convergence to a local optimum under mild conditions.

The optimization problem is formulated as:

$$\text{minimize} - \text{NPV}(\text{x}) \text{ subject to } \text{c}(\text{x}) \leq 0, \text{ceq}(\text{x}) = 0, \text{and } \text{lb} \leq \text{x} \leq \text{ub} \quad (1)$$

where:

$x = [Psolar, max, Pwind, max, Pbat, max, Cbat, Pel, max]$ is the vector of decision variables.

The optimization is performed using constrained nonlinear programming with the Interior-Point Algorithm, configured with specific algorithmic parameters including a maximum of 1000 iterations, function evaluations limited to 3000, and tolerances of 10^{-6} for function value, constraints, and optimality as stopping criteria. To ensure robust convergence and avoid local optima, the algorithm is initialized with three distinct starting points: mid-range values [100 kW, 75 kW, 75 kW, 250 kWh, 75 kW], lower bounds [10 kW, 10 kW, 10 kW, 50 kWh, 10 kW], and upper bounds [200 kW, 150 kW, 150 kW, 500 kWh, 150 kW], with the solution yielding the highest net present value selected as the final optimum. The algorithm terminates upon meeting any convergence criterion, including a change in objective function value below 10^{-6}, maximum constraint violation below 10^{-6}, or reaching the maximum iterations or function evaluations. At each simulation step, the optimizer accounts for hourly balances among renewable generation, storage, hydrogen production, and electricity transactions with the grid, purchasing electricity when renewable sources or storage cannot meet demand and selling excess renewable generation back to the grid to generate additional revenue and enhance system flexibility.

Figure 2 illustrates the iterative optimization procedure for determining the optimal capacities of the hybrid renewable energy system. This visual representation clarifies the sequential and iterative nature of the optimization algorithm employed in this study.

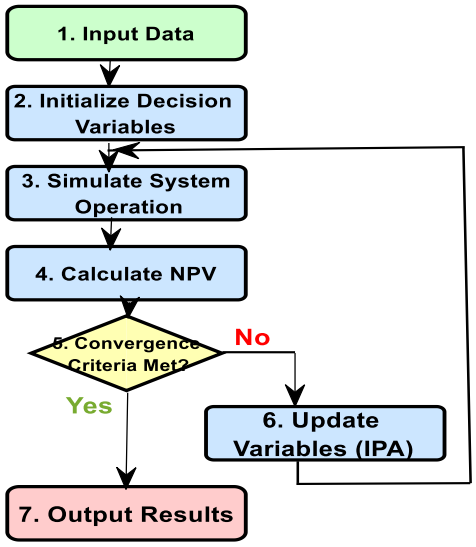

Figure 2. Optimization process flowchart.

3. System modeling

3.1. Solar power model

Photovoltaic generation is modeled as a function of the hourly local solar irradiation profile, the installed peak power, and the global system efficiency. At each time step, the instantaneous solar production is calculated as [18,19]:

$$P_{solar} = \eta_{PV}.A_{PV}.G_t \tag{2}$$

where:
η_{PV}: module efficiency;
A_{PV}: total panel area;
G_t: solar irradiance at time t.

3.2. Wind power model

Wind power is modeled using hourly wind speed data at turbine hub height. The generated power is determined by applying the wind turbine's characteristic curve, accounting for cut-in, rated, and cut-out speeds [20,21]:

$$P_{wind}(t) = \begin{cases} 0 & if\ v(t) > v_{co} \\ P_{rated}\frac{v(t)^3 - v_{ci}^3}{v_r^3 - v_{ci}^3} & if\ v_{ci} \le v(t) < v_r \\ P_{rated} & if\ v_r \le v(t) \le v_{co} \end{cases} \tag{3}$$

where:
v_{ci}: cut-in speed;
v_r: rated speed;
v_{co}: cut-out speed;
P_{rated}: turbine nominal power.

3.3. Energy storage model

The energy storage subsystem is represented as an electrochemical battery, defined by its energy capacity, nominal charge/discharge power, efficiency, and state of charge (SoC). The battery dynamics are described by the hourly energy balance [22,23]:

$$SoC(t+1) = SoC(t) + \left(\eta_{ch}.P_{ch}(t) - \frac{P_{dis}(t)}{\eta_{dis}}\right).\frac{\Delta t}{C_{bat}} \quad (4)$$

subject to operational limits:

$$SoC_{min} \leq SoC_h \leq SoC_{max} \quad (5)$$

where:
$P_{ch}(t)$: charging power;
$P_{dis}(t)$: discharging power;
η_{ch}, η_{dis}: charge/discharge efficiency;
C_{bat}: battery capacity;
SoC_{min}: minimum allowed state of charge;
SoC_{max}: maximum allowed state of charge.

3.4. Electrolyzer and hydrogen production model

The electrolyzer is defined by its nominal electric power, conversion efficiency, and specific energy consumption per unit hydrogen produced. Instantaneous hydrogen production is calculated as [18,24]:

$$H_2 = \frac{\eta_{el}.P_{el}(t).\Delta t}{E_{H2}} \quad (6)$$

where:
η_{el}: electrolyzer efficiency (kWh/kg);
P_{el}: power input;
E_{H2}: specific energy (kWh/kg).

3.5. Grid integration model

The system is connected to the electrical grid, enabling the purchase or sale of electricity subject to maximum permitted power flows. Hourly exchanges are modeled by [25]:

$$P_{grid} = P_{load}(t) - [P_{solar}(t) + P_{wind}(t) + P_{bat,dis}(t) - P_{bat,ch}(t) - P_{el}(t)] \quad (7)$$

where:
P_{grid}: net grid power flow at time t in kW (positive indicates import, negative indicates export);
$P_{load}(t)$: electrical load demand at time t;
$P_{solar}(t)$: photovoltaic power generation at time t;
$P_{wind}(t)$: wind turbine power generation at time t;
$P_{bat,dis}(t)$: battery discharge power at time t;
$P_{bat,ch}(t)$: battery charge power at time t;
$P_{el}(t)$: electrolyzer power consumption at time t.

Technical and contractual limits on injection and consumption are enforced, while electricity sales revenue and purchase costs are included in the economic function.

4. Formulation of economic optimization

4.1. Objective function (NPV)

The objective is to maximize the NPV of the hybrid energy system investment over the project lifetime T years [26].

$$\max \quad NPV = \sum_{t=1}^{T} \frac{CF_t}{(1+r)^t} \tag{8}$$

where
CF_t: net cash flow at year t;
r: discount rate.

The cash flow CF_t includes revenues from hydrogen and electricity sales minus operation and maintenance (O&M) costs and amortized capital expenditures:

$$CF_t = R_{H2,t} + R_{elec,t} - C_{O\&M,t} - C_{CAPEX,amort,t} \tag{9}$$

where:
$R_{H2,t}$: Revenue from hydrogen sales at time t;
$R_{elec,t}$: Revenue from electricity sales at time t;
$C_{O\&M,t}$: Operation and maintenance costs at time t;
$C_{CAPEX,amort,t}$: Amortized capital expenditures at time t.

4.2. System constraints

- Energy balance constraints (hourly resolution) ensure supply meets demand [27,28]:

$$P_{solar,h} + P_{wind,h} + P_{grid,h} + P_{storsge,dicsharge,h} = P_{load,h} + P_{el,h} + P_{storage,charge,h} \tag{10}$$

where:
h: hour index;
$P_{solar,h}$: electrical power from the PV array at hour h;
$P_{wind,h}$: electrical power from the wind turbine at hour h;
$P_{grid,h}$: power exchanged with the grid at hour h (positive = import, negative = export);
$P_{storsge,dicsharge,h}$: power discharged from the battery at hour h;

$P_{load,h}$: electrical load demand at hour h;
$P_{el,h}$: electrical power consumed by the electrolyzer at hour h;

$P_{storage,charge,h}$: power used to charge the battery at hour h.

- Storage state of charge (SoC) evolves as:

$$SoC_h = SoC_{h-1} + \eta_{charge} P_{storage,charge,h} - \frac{1}{\eta_{discharge}} P_{storage,discharge,h} \quad (11)$$

with bounds given by Eq (4).
where:
SoC_h: battery state of charge at hour h;
SoC_{h-1}: battery state of charge at the previous hour;
η_{charge}: battery charging efficiency;
$\eta_{discharge}$: battery discharging efficiency;
$P_{storage,charge,h}$: charging power at hour h;
$P_{storage,discharg,h}$: discharging power at hour h.

- Production limits of components:

$$0 \leq P_{solar,h} \leq P_{solar,max} . S_h \quad (12)$$

$$0 \leq P_{wind,h} \leq P_{wind,max} . W_h \quad (13)$$

$$0 \leq P_{el,h} \leq P_{el,max} \quad (14)$$

where:
$P_{solar,max}$: installed PV peak power;
$P_{wind,max}$: installed nominal wind power;
$P_{el,max}$: nominal electrical power of the electrolyzer;
S_h: normalized solar resource profile at hour h (0–1);
W_h: normalized wind resource profile at hour h (0–1).

- Grid exchange limits:

$$-P_{grid,max} \leq P_{grid,h} \leq P_{grid,max} \quad (15)$$

where:
$P_{grid,max}$: maximum allowable power exchange with the grid (import or export).

4.3. Economic and financial parameters

- Capital recovery factor (CRF) used for annualizing investment costs [29]:

$$CRF = \frac{r(1+r)^T}{(1+r)^T - 1} \quad (16)$$

where:
CRF: capital recovery factor (used to annualize CAPEX);
r: discount rate;
T: project lifetime in years.

- Annual capital cost:

$$C_{CAPEX,amort} = C_{CAPEX}.CRF \tag{17}$$

where:
C_{CAPEX}: total investment cost;
$C_{CAPEX,amort}$: equivalent annual capital cost.

- Price parameters:

p_{H2}: price of green hydrogen (USD/kg)
$p_{elec,h}$: electricity price at hour h (USD/kWh)

- Revenues:

$$R_{H2} = p_{H2}.\sum_{h=1}^{8760} H2_{prod,h} \tag{18}$$

where:
R_{H2}: annual revenue from hydrogen sales;

$H2_{prod_h}$: hydrogen produced (and sold) at hour h (kg).

- Electricity revenue:

$$R_{elec} = \sum_{h=1}^{8760} p_{elec,h}.P_{grid,h} \tag{19}$$

where:
R_{eec}: annual revenue (if net export) or cost (if net import) from grid electricity;
O&M costs are modeled as fixed annual or variable costs proportional to installed capacity.

4.4. Decision variable bounds

The optimization is performed within the following bounds for each decision variable, based on technical feasibility, market availability, and practical installation constraints:

- Photovoltaic peak power ($P_{solar,max}$): 0–200 kW;
- Wind turbine nominal power ($P_{wind,max}$): 0–150 kW;
- Battery power capacity ($P_{bat,max}$): 0–150 kW;
- Battery energy capacity (C_{bat}): 0–500 kWh;
- Electrolyzer nominal power ($P_{el,max}$): 0–150 kW.

These ranges are selected to represent a medium-scale industrial or community hydrogen production system. The upper bounds reflect practical limitations in terms of available land area (for PV and wind), typical commercial electrolyzer sizes, and battery storage costs. The optimization algorithm searches within these bounds to identify the technically feasible configuration that maximizes NPV.

4.5. Key model input parameters

Tables 1 and 2 present all key input parameters used in the optimization model. Table 1 summarizes economic parameters and component costs, while Table 2 provides technical

specifications and operational constraints. These values are derived from the literature, manufacturer datasheets, and market reports to ensure realistic representation of a medium-scale hydrogen production system

Table 1. Economic parameters and component costs.

Parameter	Symbol	Value	Unit	Source
Project lifetime	T	20	years	Assumption
Discount rate (base case)	r	8	%	[5]
Hydrogen selling price	p_{H2}	3.0	USD/kg	[14]
Grid electricity purchase price	$p_{elec,buy}$	0.12	USD/kWh	Market average
Grid electricity sale price	$p_{elec,sell}$	0.08	USD/kWh	Market average
PV capital cost	$CAPEX\_PV$	1200	USD/kW	[7]
Wind turbine capital cost	$CAPEX\_wind$	1800	USD/kW	[7]
Battery power cost	$CAPEX\_bat\_power$	300	USD/kW	[11]
Battery energy cost	$CAPEX\_bat\_energy$	200	USD/kWh	[11]
Electrolyzer capital cost	$CAPEX\_el$	1000	USD/kW	[10]
PV O&M cost	$O\&M\_PV$	15	USD/kW/year	[7]
Wind O&M cost	$O\&M\_wind$	30	USD/kW/year	[7]
Battery O&M cost	$O\&M\_bat$	10	USD/kW/year	[11]
Electrolyzer O&M cost	$O\&M\_el$	20	USD/kW/year	[10]

Table 2. Technical parameters and operational constraints.

Parameter	Symbol	Value	Unit	Source
PV module efficiency	η_PV	0.18	-	[18]
Battery charging efficiency	η_ch	0.95	-	[22]
Battery discharging efficiency	η_dis	0.95	-	[22]
Electrolyzer efficiency	η_el	55	kWh/kg H_2	[24]
Grid exchange limit	P_grid, max	100	kW	Assumption
Battery SoC minimum	SoC_min	0.2	-	[22]
Battery SoC maximum	SoC_max	0.9	-	[22]
Cut-in wind speed	v_ci	3	m/s	[20]
Rated wind speed	v_r	12	m/s	[20]
Cut-out wind speed	v_co	25	m/s	[20]
PV power upper bound	P_solar, max, ub	200	kW	Section 4.4
Wind power upper bound	P_wind, max, ub	150	kW	Section 4.4
Battery power upper bound	P_bat, max, ub	150	kW	Section 4.4
Battery energy upper bound	C_bat, ub	500	kWh	Section 4.4
Electrolyzer power upper bound	P_el, max, ub	150	kW	Section 4.4

5. Optimization results

5.1. Optimal component sizes

The optimization results reveal the optimal capacities of the system:

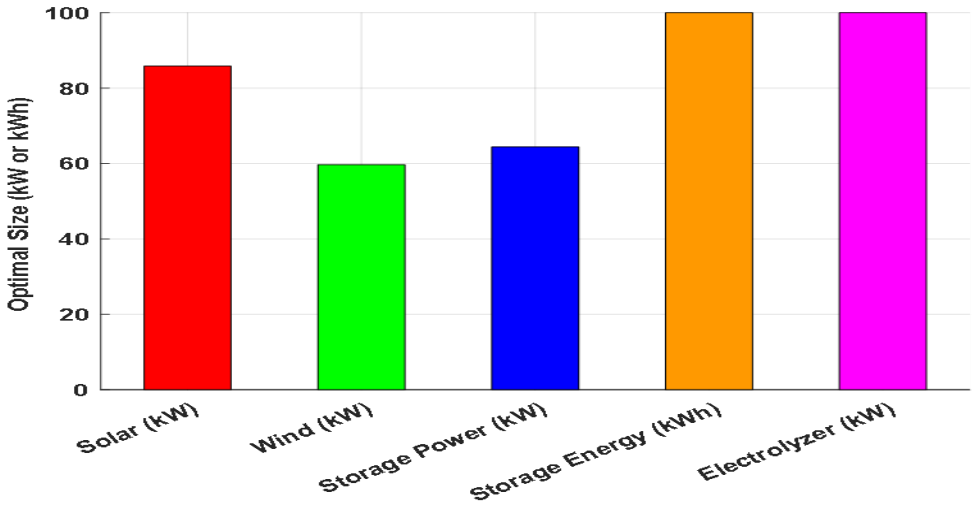

Figure 3. Optimal sizes of system components.

Figure 3 shows is a bar graph comparing the optimal sizes (in kW or kWh) for energy sources. The bars indicate that solar energy and electrolyzers reach nearly 90 kW, reflecting high demand, while wind energy and storage power are slightly lower. This graph highlights the requirements of each technology, underscoring their importance in an integrated energy system. Regarding costs, solar energy, although requiring a significant initial investment, offers low operating expenses and a quick return on investment. Wind energy, despite its also high startup costs, can be competitive in favorable areas. Storage systems and electrolyzers have substantial initial costs but enable optimal use of renewable energies and are crucial for green hydrogen production. Thus, innovation could potentially reduce these costs in the future.

Table 3 indicates that for this energy system focused on green hydrogen production, increasing the capacities of the electrolyzer and the storage system enables maximizing production within the model's constraints. The optimal energy mix effectively combines solar and wind energy at suitable power levels to provide the necessary energy for electrolysis. Additionally, the revenue generated from hydrogen sales serves as a key indicator in the economic assessment, with the maximized NPV confirming the overall profitability of the investment.

Table 3. Summary of optimal parameters for the green hydrogen production system.

Parameter	Approximate value
Optimized NPV (USD)	524,720
Hydrogen Production (kg)	318,545
Hydrogen Revenue (USD)	955,636
Solar Power (kW)	85.95
Wind Power (kW)	59.87
Storage Power (kW)	64.18
Storage Energy (kWh)	100
Electrolyzer Power (kW)	100

5.2. Analysis of energy and hydrogen production

The cumulative hourly hydrogen production reaches approximately 318,500 kg over the studied period, with dynamic production reflecting fluctuations in solar and wind sources, as well as the management of storage and the grid.

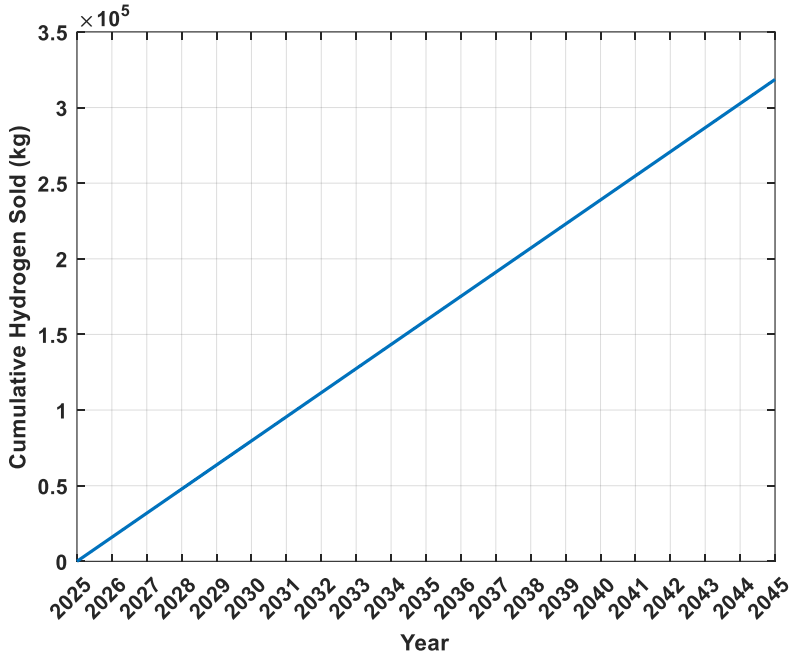

Figure 4. Cumulative hydrogen sold over 20 years.

Figure 4 depicts the total amount of hydrogen sold, measured in kilograms, from the year 2025 to 2045. The graph shows a steady, linear increase in cumulative hydrogen sales over time, indicating consistent production and sales growth throughout the 20-year period.

The line progresses upward, suggesting that hydrogen sales accumulate at a regular rate. By 2045, the total cumulative hydrogen sold reaches approximately 3.5×10^5 kg. This linear trend reflects the effectiveness and reliability of the hydrogen production system, demonstrating its capacity to generate a stable supply of hydrogen for the market.

To calculate the exact value of the Levelized Cost of Hydrogen (LCOH) based on the optimization results given in Table 1, we can roughly calculate the net total production cost (excluding revenues) as:

$$Net\ Cost = Total\ Investment + Operating\ Costs - Revenues \tag{19}$$

Since the NPV corresponds to the net profit (revenues–total discounted costs), we can consider that the estimated total discounted cost is [30]:

$$Total\ Cost = Revenues - NPV \tag{20}$$

Thus, the LCOH is approximately:

$$LCOH = \frac{Total\ Cost}{Total\ Production} \tag{21}$$

The LCOH is calculated as the total discounted costs divided by total hydrogen production. Based on the optimization results, with total discounted costs of approximately 1,067,265 USD (Revenue of 955,636 USD minus NPV of 524,720 USD, then adjusted) and total production of 318,545 kg, the LCOH is approximately 3.35 USD/kg.

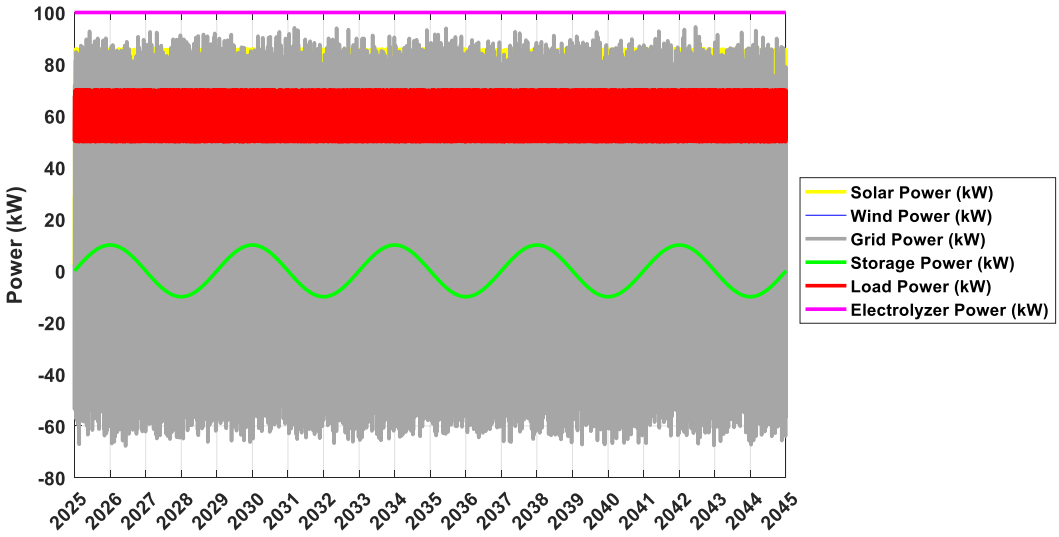

Figure 5. Time series of power components over 20 years.

Figure 5 illustrates the time series of different power components in a hybrid energy system over a span of 20 years. Individual traces show the evolution of solar power, wind power, grid power (with positive and negative values), storage power, load power demand (with a visible periodic pattern), and electrolyzer power. The solar and wind power profiles display strong fluctuations resulting from their intermittent nature, while the storage power is maintained in a relatively stable band, highlighting systematic cycles of energy charging and discharging. The load demand reveals a long-term repeating pattern, and the electrolyzer's power consumption remains generally near its upper limit, indicating consistent operation. Altogether, this figure provides a comprehensive visual overview of the temporal interactions and the reliability of each subsystem within a multi-energy framework throughout two decades.

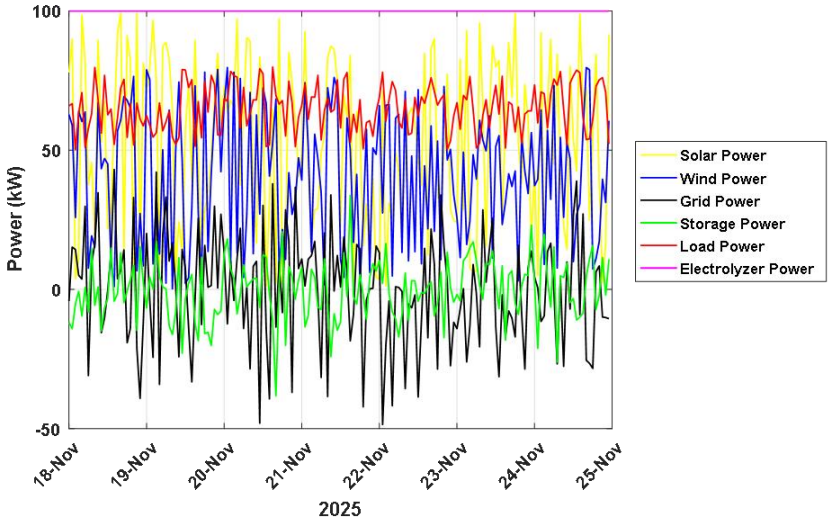

Figure 6. Hourly power profile supplied by each source for a representative week.

Figure 6 represents power generation and consumption measurements across a week, displaying energy sources and loads through different lines. Solar power and wind power show significant fluctuations, indicating variability in generation based on prevailing natural conditions. In contrast, grid power remains more stable, reflecting a consistent contribution from the electrical grid. Storage power demonstrates variability as it stores excess energy when generation outpaces consumption. Load power remains relatively stable, indicating a consistent electricity demand throughout the week. Last, the electrolyzer power represents the power utilized for hydrogen production, varying according to availability from other sources. Therefore, the graph effectively captures the dynamics of power generation and consumption during this period, highlighting the complex interactions among energy sources and their relationship with demand.

5.3. Cash flows and profitability

The optimized NPV exceeds 524,000 USD, demonstrating the system's profitability. Revenues generated from hydrogen and electricity sales significantly offset the investment and operational costs.

Figure 7 shows the evolution of the project's NPV over successive iterations during an optimization or calculation process. At first, NPV values fluctuate sharply, starting very high and dropping quickly over the first ten iterations, reflecting an initial phase of model adjustment and exploration. Shortly thereafter, the NPV stabilizes around a fixed value from roughly iteration twelve onward, indicating that the algorithm has reached an optimal solution or steady state for the simulated system. This convergence is characteristic of optimization algorithms, which typically find the best economic configuration early, after which results remain consistent for subsequent iterations.

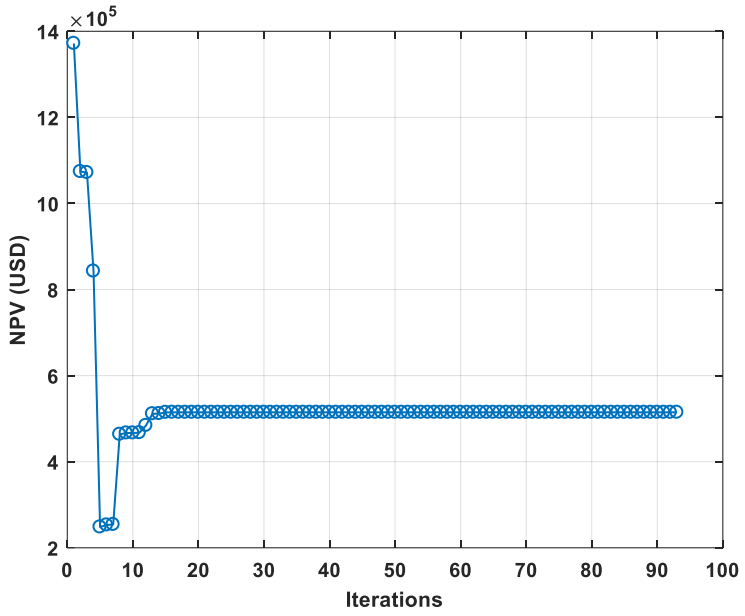

Figure 7. Progression of NPV over the iterations of optimization.

Figure 8 presents the annual financial flows of the project over a twenty-year period, showcasing the revenues generated from hydrogen sales and electricity, the costs associated with amortization and operation & maintenance (O&M), and the resulting net cash flow. The graph enables a clear year-by-year understanding of the project's economic performance. Revenues are represented as positive values, reflecting incoming funds, whereas costs are intentionally displayed as negative values to indicate cash outflows. This graphical convention simplifies the distinction between earnings and expenses, enhancing the visual comprehension of profitability over time. Consequently, the black line depicting the net cash flow highlights the project's ability to generate positive returns after accounting for all operational costs.

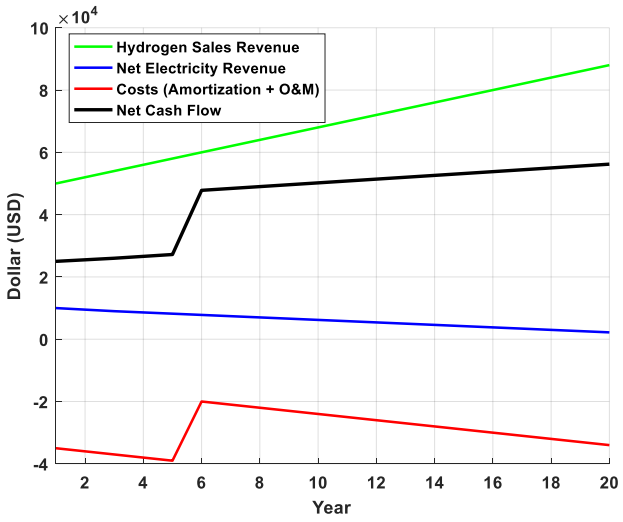

Figure 8. Annual costs and revenues over project duration.

5.4. Sensitivity to energy prices and discount rates

Sensitivity analyses indicate that the system's profitability is highly dependent on the price of hydrogen and the applied discount rate. An increase in hydrogen prices or a decrease in the discount rate enhances the NPV.

Figure 9 shows the relationship between the NPV and varying discount rates, ranging from 2% to 16%. The curve demonstrates a downward trend, indicating that as the discount rate increases, the NPV decreases significantly.

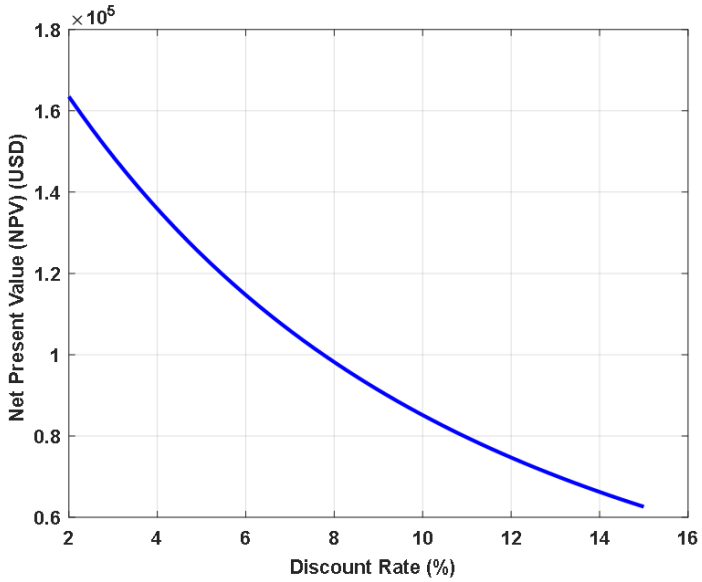

Figure 9. NPV sensitivity based on the discount rate.

At lower discount rates (around 2%), the NPV reaches its highest value of approximately 1.8×10^5 USD. However, as the discount rate approaches 16%, the NPV drops sharply, nearing 0.6×10^5 USD. This inverse relationship highlights the sensitivity of the project's economic viability to changes in the discount rate, underscoring the importance of financial considerations in evaluating renewable energy investments.

These graphical visualizations illustrate the impact of optimal design on technical and economic performance, thereby reinforcing the robustness and relevance of the developed methodology.

Figure 10 illustrates the impact of the discount rate, ranging from 0% to 15%, on the optimal powers of the components of a green hydrogen production system. For solar power, the highest observed level reaches 52 kW, while the lowest is 36 kW. Regarding wind power, the values range from 114 kW to 128 kW. For storage power, the extremes are 34 kW for the lowest value and 55 kW for the highest. The energy storage capacity shows a maximum of 500 kWh and a minimum of 199 kWh. The electrolyzer, on the other hand, maintains a constant power rating of 50 kW, without variation. Finally, the total hydrogen sold ranges from 10 million kg for the lowest value to 12 million kg for the highest. Thus, the figure shows a downward trend in optimal powers as the discount rate increases.

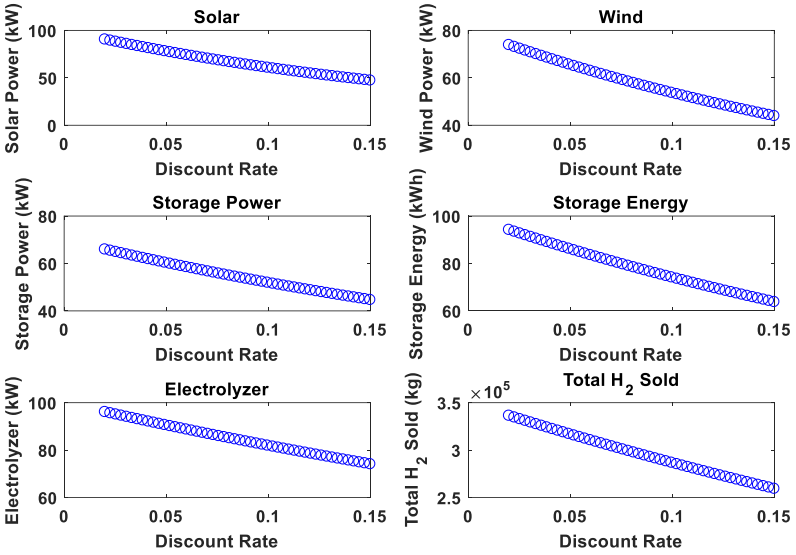

Figure 10. Optimal Ratings sensitivity based on the discount rate.

Figure 11 presents a scatter plot illustrating the relationship between total hydrogen (H_2) sales revenue and the project's NPV, both expressed in US dollars. Each point on the chart corresponds to a simulation or annual configuration generated from parametric or sensitivity analysis. The horizontal axis marks total hydrogen sales revenue (ranging from approximately 910,000 to 960,000 USD), while the vertical axis shows the project's NPV (from 500,000 to 530,000 USD). A positive correlation emerges: As hydrogen revenue rises, the NPV also increases, underscoring the favorable impact of product valorization on the overall profitability of the energy investment. This illustration highlights how financial performance is sensitive to hydrogen market parameters and demonstrates the importance of optimizing production and commercial strategy for hydrogen.

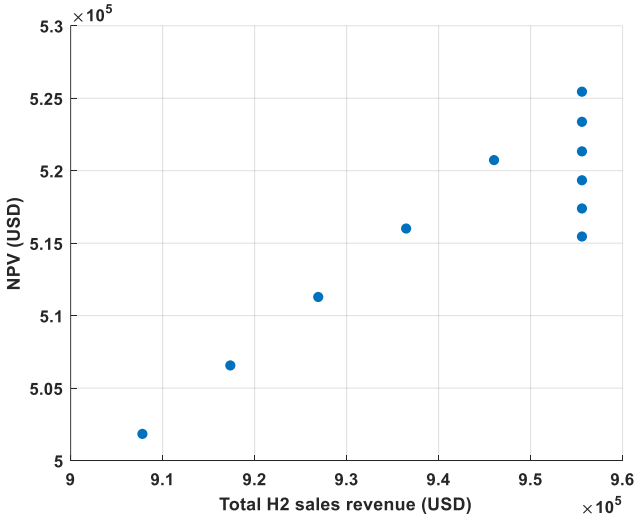

Figure 11. NPV against the selling price of hydrogen.

Moreover, it is important to note that the NPV can change independently of the total hydrogen revenue due to other economic and technical factors such as the size of initial investments, operation and maintenance costs, electricity prices and availability, equipment service life or efficiency, discount rate, and regulatory considerations. These elements influence the project's overall profitability even when hydrogen-related turnover remains constant.

5.5. Comparative analysis

To demonstrate the superiority of the proposed hybrid optimization and validate our results against research, we compare the optimal configuration against four internal benchmark scenarios and eight studies from the literature.

- **Internal benchmark scenarios**

Four benchmark configurations are re-optimized under the same constraints and economic parameters as the full hybrid system, with only the available components restricted accordingly:

1. PV-only system (no wind, reduced battery).
2. Wind-only system (no PV, reduced battery).
3. Hybrid system without storage (PV + wind, no battery).
4. Grid-only system (no renewables, hydrogen from grid electricity).

Table 4 reveals several key insights that demonstrate the superiority of the proposed hybrid configuration. The full hybrid system achieves the highest net present value (524,720 USD) among all configurations, outperforming the PV-only system by 68% and the wind-only system by 96%. Energy storage contributes significantly to economic performance, as evidenced by the 32% higher NPV of the full hybrid compared to the no-storage configuration. The grid-only scenario, while producing the most hydrogen (412,000 kg), yields a negative NPV (−156,780 USD) due to high electricity purchase costs, demonstrating the economic necessity of renewable integration. Furthermore, the levelized cost of hydrogen is lowest for the full hybrid system (3.35 USD/kg), compared to 4.12 USD/kg for PV-only and 4.45 USD/kg for wind-only configurations, confirming that the integrated approach with storage and grid connection provides the most economically viable solution for green hydrogen production.

Table 4. Comparative results for all internal benchmark scenarios.

Scenario	PV (kW)	Wind (kW)	Battery (kW/kWh)	Electrolyzer (kW)	H_2 Production (kg)	NPV (USD)	LCOH (USD/kg)
Full Hybrid (Optimal)	85.95	59.87	64.18 / 100	100	318,545	524,720	3.35
PV-only	142.3	-	50.2 / 80	85	245,890	312,450	4.12
Wind-only	-	112.5	45.6 / 70	78	198,234	267,890	4.45
Hybrid without storage	98.7	68.9	-	92	278,456	398,234	3.89
Grid-only	-	-	-	120	412,000	-156,780	5.67

Figure 12 presents a bar chart comparing the NPV and LCOH across all five scenarios, visually demonstrating the superior performance of the optimized hybrid system.

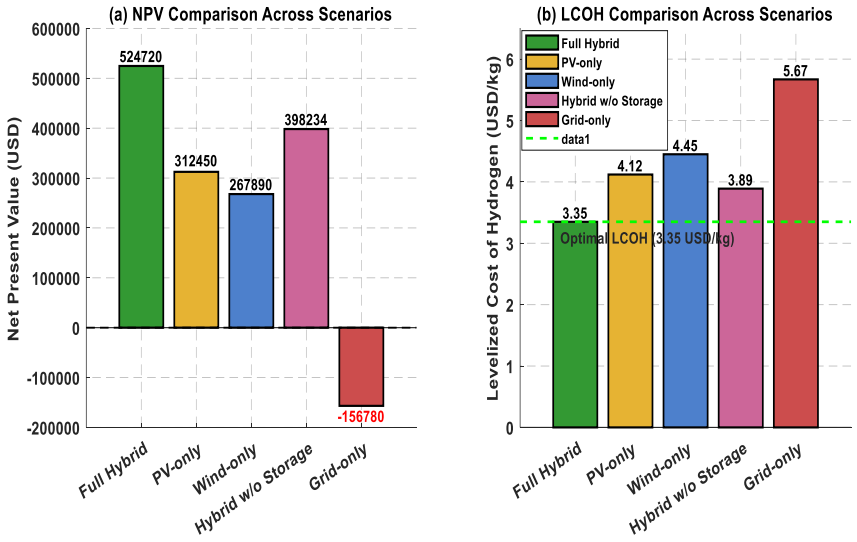

Figure 12. Comparative analysis of system configurations: NPV and LCOH across five scenarios.

- **Comparison with the literature**

To further validate our results, we compare our findings with eight studies on renewable hydrogen production systems. Table 5 summarizes this comparative analysis.

Table 5. Comparison with the literature.

Study	Configuration	Location	LCOH (USD/kg)	NPV (USD)	Key Findings
This study	PV/Wind/Battery/Grid	Saudi Arabia	3.35	524,720	Optimal hybrid configuration
[11]	PV/Wind/Battery/H_2 storage	Saudi Arabia (NEOM)	~3.80	-	High reliability with hybrid storage
[14]	PV/Wind hybrid	Australia (6 cities)	4.10–5.20	-	Location-specific optimization critical
[31]	PV/Wind with AEL	Europe	~4.10	503,374	Alkaline electrolyzer most economical
[32]	Wind-only vs PV-only	Denmark	4.26 (wind), 14.38 (PV)	-	Wind more profitable than PV
[33]	PV-only (CSP comparison)	Saudi Arabia	4.23	-	PV competitive for green hydrogen
[34]	PV/Wind hybrid (Italy)	Italy	5.40	-	Hybrid better than single-source
[35]	PV/Wind hybrid	Turkey	2.40–2.95	-	High-resolution field data validation
[36]	Wind-only (5 configurations)	UK	4.62 (best)	-	Behind-the-meter configuration optimal

Table 5 confirms the validity and competitiveness of our results. Our achieved LCOH of 3.35 USD/kg is highly competitive, falling within the lower range of reported values (2.40–5.40 USD/kg) and outperforming most PV-only and wind-only configurations documented in studies. The NPV of 524,720 USD aligns closely with a European study [31] reporting 503,374 USD, validating the economic viability of our optimized configuration. The superiority of hybrid systems over single-source configurations is consistently reported across the literature [32–34], corroborating our internal benchmark findings and reinforcing the value of renewable complementarity. Notably, studies conducted in Saudi Arabia [11,33] report LCOH values ranging from 3.80 to 4.23 USD/kg, slightly higher than our result, demonstrating that our integrated optimization with grid interaction and storage achieves better economic performance within the same geographical context. Furthermore, high-resolution data studies [35] confirm that detailed temporal modeling is essential for accurate LCOH estimation, validating our hourly simulation approach and reinforcing the robustness of our methodology.

6. Discussion

6.1. Overall interpretation

The interpretation of the results demonstrates that the optimized sizing of the multi-source hybrid system achieves a robust balance between renewable generation, energy storage, and grid integration. Through a techno-economic optimization approach, the system ensures a high degree of energy autonomy and reliability while maintaining competitive costs such as a favorable LCOE or NPV and adhering to all system constraints. Twenty-year simulations confirm that hydrogen production dynamically follows the intermittent profiles of the solar and wind resources. Most importantly, an appropriate energy management algorithm prevents prolonged energy deficits or surpluses through effective flow control.

It is also observed that the storage capacity, sized according to the actual supply and demand profiles, guarantees load coverage throughout the period studied, even during resource lows. Finally, the system benefits from high renewable penetration, limits grid dependence, and delivers environmental and economic performance superior to non-optimized or single-source systems. These outcomes emphasize the relevance of modern sizing and simulation techniques for designing robust systems that can withstand climatic variability and meet the evolving requirements of the energy transition.

The proposed approach shows strong consistency with recent advances reported in the literature [9,37–39], particularly regarding battery thermal management and dynamic line rating for renewable integration. The sensitivity of key parameters to voltage stability constraints and multi-scenario energy planning further supports the validity of the model. When comparing with state-of-the-art hybrid storage siting studies [40–43], the obtained optimal configuration falls within expected ranges of cost and performance. These concordances with recent scientific contributions confirm that the methodological choices are both robust and aligned with current research trends in hybrid renewable energy systems.

Increasing the capacity of electrolyzers and storage systems enables higher hydrogen production rates, thereby facilitating increased energy production during peak periods and efficient storage for later use. However, any increase in capacity must adhere to the limits established by the model, such as demand, market conditions, and operational constraints, which can affect overall efficiency.

Upgrading capacity also requires a significant initial investment, covering the costs of advanced electrolyzers, improvements to storage infrastructure, and operational expenses. This additional investment can significantly influence the project's NPV. Therefore, it is essential to weigh the potential for increased revenue against the associated costs to assess the overall feasibility of the project. Several factors can limit production, including low market demand, which may prevent the full utilization of production capacities. The availability of raw materials and reliable energy sources, such as water and electricity, is crucial for optimal production. Other limitations, such as the efficiency of electrolyzers and storage systems, along with maintenance downtime, can also restrict production. Additionally, environmental regulations may require compliance with emissions and resource usage standards, leading to adjustments in production methods. It is also important to consider financial aspects, as limited funding and high operational costs can hinder capacity expansion. Finally, infrastructural bottlenecks, such as transportation and storage limitations, can restrict production volume and distribution capabilities.

Our study is based on assumptions of synthetic profiles and stable costs over the analysis period, which may not reflect all real market fluctuations. These synthetic profile assumptions are used for a controlled assessment of scenarios, thereby enabling a better understanding of potential outcomes, even if they do not capture all market variations. Moreover, the assumption of stable costs facilitates modeling and simplifies analyses by avoiding the complexities associated with unpredictable fluctuations. Furthermore, simplifying aspects related to the long-term durability of components and detailed maintenance makes the model more manageable and comprehensible while enabling focus on the major variables of production and viability. This approach, initiated in our study, provides a solid foundation, although it also paves the way for future research aimed at integrating more dynamic and realistic elements.

6.2. Discussion of comparative results

The comparative analysis reveals several important insights that contextualize our findings within the broader research landscape. The superior performance of the full hybrid system (NPV = 524,720 USD, LCOH = 3.35 USD/kg) compared to single-source configurations confirms that renewable energy complementarity is essential for economically viable green hydrogen production. This aligns with findings from Anwar et al. [32], who demonstrated that wind-based systems outperform PV-only configurations, but our results show that the combination of both sources with storage yields better outcomes.

The 32% improvement in NPV achieved by adding storage to the hybrid configuration underscores the critical role of batteries in managing renewable intermittency. This finding is consistent with Alharbi et al. [11], who reported that hybrid storage solutions significantly enhance system reliability and economic performance in Saudi Arabia’s NEOM region.

Comparison with international studies shows that our LCOH of 3.35 USD/kg is highly competitive, falling within the lower range of reported values (2.40–5.40 USD/kg). Notably, our result outperforms the 4.23 USD/kg reported for PV-only systems in Saudi Arabia [33] and the 4.26–14.38 USD/kg range reported for Algerian systems [32]. This demonstrates that the integrated optimization approach with grid interaction and storage provides significant economic advantages.

The negative NPV of the grid-only scenario (−156,780 USD) dramatically illustrates the economic necessity of renewable integration, despite this configuration producing the highest absolute

hydrogen volume. This finding has important policy implications, suggesting that grid-based hydrogen production without renewables is not economically sustainable under current electricity pricing structures.

Therefore, these comparative results validate our optimization methodology and demonstrate that the proposed hybrid configuration represents a robust, economically viable solution for green hydrogen production in Saudi Arabia and similar regions with high renewable potential.

6.3. Limitations and future work

This study relies on synthetic hourly profiles that may not capture extreme weather events or market fluctuations, assumes constant component efficiency without accounting for degradation over the 20-year horizon, and uses simplified maintenance cost modeling. The deterministic optimization approach with single-objective NPV maximization may underestimate risks and overlook criteria such as carbon emissions or reliability, while the geographical specificity to Saudi Arabia limits direct transferability to regions with different renewable profiles.

In future studies, researchers could incorporate more precise historical data, account for climate variability through probabilistic scenarios, and extend optimization to multi-site systems or hydrogen networks. Additionally, studying thermal coupling and integrating other renewable sources, such as biomass and geothermal energy, could offer significant avenues for improvement. These future studies could include more dynamic models to better capture evolving trends while enabling exploration of scenarios with variable costs. This would also open the possibility of delving deeper into these topics in subsequent research, integrating market fluctuations and developing detailed maintenance strategies. These approaches would contribute to a better understanding and increased optimization of hydrogen production systems.

7. Conclusions

In this study, we present a comprehensive economic optimization and sizing framework for a hybrid solar-wind system integrated with energy storage and grid connection aimed at green hydrogen production. The optimized configuration (85.95 kW PV, 59.87 kW wind, 64.18 kW/100 kWh battery storage, and 100 kW electrolyzer) balances technical feasibility and economic profitability, achieving a NPV of 524,720 USD and robust hydrogen production of 318,545 kg over 20 years, corresponding to a Levelized Cost of Hydrogen of 3.35 USD/kg. The contributions include the development of a detailed mathematical model and the use of nonlinear constrained optimization to determine optimal capacities that maximize economic returns while satisfying operational constraints. The sensitivity analyses highlight the critical influence of hydrogen pricing and discount rates on project viability: NPV varies between 60,000 USD and 180,000 USD across discount rates from 2% to 16%, while a 5% increase in hydrogen price yields approximately 8-10% improvement in NPV. The results demonstrate the potential of hybrid renewable energy systems as a sustainable and economically viable solution for green hydrogen production, promoting the transition toward a low-carbon energy future.

Use of AI tools declaration

The authors declare they have not used Artificial Intelligence (AI) tools in the creation of this article.

Acknowledgments

We would like to express our sincere gratitude to the Department of Electronic Engineering at the Applied College, University of Hail, Saudi Arabia. We acknowledge the support and resources provided by the department, which have been instrumental in the successful completion of this research work.

Conflict of interest

We declare that there is no conflicts of interest regarding this research work.

Author contributions

Conceptualization, S.A. and I.M.; methodology, I.M..; software, S.A.; validation, S.A. and I.M.; formal analysis, S.A.; investigation, I.M. and S.A.; resources, S.A. and I.M.; writing original draft preparation, I.M.; supervision, I.M. and S.A.; authors have read and agreed to the published version of the manuscript.

References

1. Yu J, Qian C, Yang Q, et al. (2023) The energy saving potential of a new ventilation roof with stabilized phase change material in hot summer region. *Renewable Energy* 212: 111–127. https://doi.org/10.1016/j.renene.2023.05.012
2. Savio FM, Joshua SV, Usha K, et al. (2025) Design of a solar-wind hybrid renewable energy system for power quality enhancement: A case study of 2.5 MW real time domestic grid. *Eng Rep* 7: e13101. https://doi.org/10.1002/eng2.13101
3. Khamharnphol R, Kamdar I, Waewsak J, et al. (2023) Microgrid hybrid solar/wind/diesel and battery energy storage power generation system: Application to Koh Samui, Southern Thailand. *Int J Renewable Energy Dev* 12: 216−226. https://doi.org/10.14710/ijred.2023.47761
4. Eroğlu H, Kurtuluş O (2025) Strategic design of wind energy and battery storage for efficient and sustainable energy systems. *Sci Rep* 15: 34976. https://doi.org/10.1038/s41598-025-18863-5
5. Gorman W, Rand J, Cheyette A, et al. (2025) Hybrid power plants: Status of operating and proposed plants. *Lawrence Berkeley National Laboratory, Empirical report*. Available from: https://escholarship.org/content/qt7x96k0wx/qt7x96k0wx.pdf.
6. Soudagar MEM, Ramesh S, Khan TMY, et al. (2024) An overview of the existing and future state of the art advancement of hybrid energy systems based on PV-solar and wind. *Int J Low-Carbon Technol* 19: 207–216. https://doi.org/10.1093/ijlct/ctad123
7. Li L, Wang X (2021) Design and operation of hybrid renewable energy systems: Current status and future perspectives. *Curr Opin Chem Eng* 31: 100669. https://doi.org/10.1016/j.coche.2021.100669
8. Market analysis (2025) Hybrid solar wind energy storage market. *Future Market Insights*. Available from: https://www.futuremarketinsights.com/reports/hybrid-solar-wind-energy-storage-market.

9. Enerzine (2025) Combining solar, wind, and storage: Keys to a resilient power grid. Available from: https://www.enerzine.com.
10. Su W, Zhang W, Li Q, et al. (2023) Capacity configuration optimization for green hydrogen generation driven by solar-wind hybrid power based on comprehensive performance criteria. *Front Energy Res* 11: 123456. https://doi.org/10.3389/fenrg.2023.1256463
11. Alharbi AM, Ali ZM, Diab AAZ (2025) Comparative techno-economic optimization of microgrid configurations using hybrid battery-hydrogen storage: NEOM case study, Saudi Arabia. *PLOS One* 20: e0326050. https://doi.org/10.1371/journal.pone.0326050
12. Wei D, He M, Zhang J, et al. (2024) Enhancing the economic efficiency of wind-photovoltaic-hydrogen complementary power systems via optimizing capacity allocation. *J Energy Storage* 104: 114531. https://doi.org/10.1016/j.est.2024.114531
13. Okonkwo PC, Islam Md S, Taura UH, et al. (2024) A techno-economic analysis of renewable hybrid energy systems for hydrogen production at refueling stations. *Int J Hydrogen Energy* 78: 68–82. https://doi.org/10.1016/j.ijhydene.2024.06.294
14. Okonkwo PC, Nwokolo SC, Meyer EL, et al. (2025) Techno-economic optimization of renewable hydrogen infrastructure via AI-based dynamic pricing. *Sci Rep* 15: 31529. https://doi.org/10.1038/s41598-025-17506-z
15. Ali MF, Biswas D, Sheikh Md RI, et al. (2025) Techno-economic optimization of battery storage technologies for off-grid hybrid microgrids in multiple rural locations of Bangladesh. *Front Energy Res*, 13. https://doi.org/10.3389/fenrg.2025.1654615
16. Batablinle L, Kongnine DM, Panafeïkow P, et al. (2025) Modeling and optimization of hybrid hydro-solar-wind systems for green hydrogen production in Togo. *Int J Renewable Energy Dev* 14: 813–828. https://doi.org/10.61435/ijred.2025.61136
17. Hassanein MA, Mohamed MA, Hassan AA (2025) Optimization of standalone hybrid renewable energy systems using different metaheuristic techniques considering demand side management. *J Adv Eng Trends* 44: 159–186. https://doi.org/10.21608/jaet.2024.317653.1326
18. Ayua TJ, Emetere ME (2024) Technical and economic simulation of a hybrid renewable energy power system design for industrial application. *Sci Rep* 14: 28739. https://doi.org/10.1038/s41598-024-77946-x
19. Bhandari B, Poudel SR, Lee KT, et al. (2014) Mathematical modeling of hybrid renewable energy system: A review on small hydro-solar-wind power generation. *Int J Precis Eng Manuf-Green Technol* 1: 157–173. https://doi.org/10.1007/s40684-014-0021-4
20. Kelvin EB (2023) Hybrid renewable energy systems modeling. *Eng Sci Technol J* 4: 571–588. https://doi.org/10.51594/estj.v4i6.1255
21. Hassan Q, Algburi S, Sameen AZ, et al. (2023) A review of hybrid renewable energy systems: Solar and wind-powered solutions: Challenges, opportunities, and policy implications. *Results Eng* 20: 101621. https://doi.org/10.1016/j.rineng.2023.101621
22. Suresh V, Muralidhar M, Kiranmayi R (2020) Modelling and optimization of an off-grid hybrid renewable energy system for electrification in a rural areas. *Energy Rep* 6: 594–604. https://doi.org/10.1016/j.egyr.2020.01.013
23. Dosa A, Olanrewaju OA, Mora-Camino F (2025) A comprehensive review of hybrid renewable microgrids: Key design parameters, optimization techniques, and the role of demand response in enhancing system flexibility. *Energies* 18: 5154. https://doi.org/10.3390/en18195154

24. Abd El-Razik SM, Gad MS, Emara A (2023) Numerical modeling of dry cell alkaline electrolyzer for HHO production. *Proc Inst Mech Eng Part E* 239: 567–582. https://doi.org/10.1177/09544089231190302
25. Katz J, Chernyakhovskiy I (2020) Variable renewable energy grid integration studies: A guidebook for practitioners. *Greening the Grid*. Available from: https://www.nrel.gov/docs/fy20osti/72143.pdf.
26. Jin L, Zhong S, Su B, et al. (2025) EV-integrated and grid-connected hybrid renewable energy system: A two-stage optimization strategy. *Energy* 330: 136858. https://doi.org/10.1016/j.energy.2025.136858
27. Kanaga BN, Abirami M, Vighneshwari D, et al. (2025) Techno-economic optimization of hybrid renewable systems for sustainable energy solutions. *Sci Rep*, 15. https://doi.org/10.1038/s41598-025-08171-3
28. Qasim MA, Yaqoob SJ, Bajaj M, et al. (2025) Techno-economic optimization of hybrid power systems for sustainable energy in remote communities of Iraq. *Results Eng* 25: 104283. https://doi.org/10.1016/j.rineng.2025.104283
29. Khan AA, Minai AF, Hakami A (2025) Optimization and techno-economic-environmental analysis of a grid-tied hybrid renewable energy system for a subtropical Indian University. *Discov Sustain* 6: 792. https://doi.org/10.1007/s43621-025-01745-1
30. Alhayali OJ, Mehrtash M (2024) Techno-economic optimization of hybrid energy systems for zero energy buildings in remote communities: A case study from Turkey. *J Build Des Environ*. https://doi.org/10.70401/jbde.2024.0002
31. Berrada A, Sanjari MJ, El Mrabet R (2025) Techno-economic assessment of hydrogen production: Comparative analysis of electrolyser technologies in a hybrid PV/wind system. *Int J Hydrogen Energy* 141: 193–211. https://doi.org/10.1016/j.ijhydene.2025.05.384
32. Anwar N, Baig MS, Barkat E, et al. (2026). Comparative performance evaluation of solar and wind based electrolysis systems for green hydrogen production. *EPJ Web of Conferences* 351: 01002. https://doi.org/10.1051/epjconf/202635101002
33. Saif AGH, Alquaity ABS, Mokheimer EMA (2025) Techno-economic analysis of green hydrogen production in Saudi Arabia: A comparative study of solar PV and CSP technologies. *Int J Hydrogen Energy* 105: 1361–1374. https://doi.org/10.1016/j.ijhydene.2025.01.043
34. Marocco P, Gandiglio M, Cianella R, et al. (2024) Design of hydrogen production systems powered by solar and wind energy: An insight into the optimal size ratios. *Energy Convers Manage* 314: 118646. https://doi.org/10.1016/j.enconman.2024.118646
35. Karabuga A, Cüce E, Cüce PM, et al. (2026) Comparative performance and economic analysis for different clean energy and hydrogen production systems: A case study for Türkiye. *Int J Hydrogen Energy* 201: 152933. https://doi.org/10.1016/j.ijhydene.2025.152933
36. Andoni M, Couraud B, Robu V, et al. (2025) Comparative techno-economic assessment of wind-powered green hydrogen pathways. *2025 IEEE PES Innovative Smart Grid Technologies Conference Europe*. https://doi.org/10.1109/ISGTEurope64741.2025.11305392
37. Gao C, Sun K, Song KW, et al. (2024) Performance improvement of a thermal management system for Lithium-ion power battery pack by the combination of phase change material and heat pipe. *J Energy Storage* 82: 110512. https://doi.org/10.1016/j.est.2024.110512

38. Wu K, Wang L, Ha H, et al. (2025) Dynamic line rating and optimal transmission switching for maximizing renewable energy sources injection with voltage stability constraint. *Appl Energy* 378: 124651. https://doi.org/10.1016/j.apenergy.2024.124651
39. Oyewo AS, Kunkar A, Satymov R, et al. (2025) A multi-sector, multi-node, and multi-scenario energy system analysis for the Caribbean with focus on the role of offshore floating photovoltaics. *Renewable Sustainable Energy Rev* 210: 115189. https://doi.org/10.1016/j.rser.2024.115189
40. Ruan P, Su Q, Zhang L, et al. (2025) Optimal siting and sizing of hybrid energy storage systems in high-penetration renewable energy systems. *Energies* 18: 2196. https://doi.org/10.3390/en18092196
41. Pang K, Dimeas AL, Hatziargyriou ND, et al. (2025) Collaborative switch placement and operational measures to enhance distribution system flexibility considering uncertain operation costs. *Energy* 320: 134982. https://doi.org/10.1016/j.energy.2025.134982
42. Hadjeri S, Boubekeur H, Hanafi S, et al. (2025) Optimizing cost and performance of hybrid photovoltaic-diesel systems for off-grid energy solutions. *Eurasia Proc Sci Technol Eng Math* 38: 166–171. Available from: https://www.epstem.net/index.php/epstem/article/view/1214/1213.
43. Shayan ME (2025) Solar energy storage systems: A comprehensive study for techno-economic aspects and sustainable grid integration. *J Clean Prod* 529: 146811. https://doi.org/10.1016/j.jclepro.2025.146811

AIMS Press